International Journal of Mechanical Engineering and Technology (IJMET)
Volume 10, Issue 2, February 2019, pp. 1640–1654, Article ID: IJMET_10_02_169
Available online at http://www.iaeme.com/ijmet/issues.asp?JType=IJMET&VType=10&IType=2
ISSN Print: 0976-6340 and ISSN Online: 0976-6359

STUDY ON AL_2O_3 DUPLEX COATINGS DEPOSITED BY NEW MICRO-ARC OXIDATION (MAO) PROCESS USING NATURAL ADDITIVES OF RICE HUSHES ASH (RHA) AND PORCELANITE ROCKS OF PRE-ANODIZED 6061 AL ALLOYS

SAMIR HAMID AWAD
University of Babylon, p.o.box:4, Hilla, Babylon, Iraq

ABSTRACT

In this study, pre anodized Al 6061 alloy was coated with protective ceramic coatings using micro- arc oxidation process (MAO). MAO electrolyte was modified using natural additives of rice hushes ash (RHA) fired at 800°C and porcelanite rocks fired at 700° C. The surface morphology, phase content, structure, and element distribution of the coatings were investigated by X-ray diffraction, scanning electron microscope, energy dispersive spectroscopy, and atomic force microscopy. Results showed that the samples coatings contained γ-alumina, and their thickness and hardness increased by the increasing of deposition time. The research demonstrates that a relatively hard, thick and uniform coatings with good wear resistance, can successfully be deposited on pre anodized Al alloy using natural additives of rice hushes ash (RHA) and porcelanite rocks containing MAO electrolytes as natural additives. The results proved that the pre anodized surfaces promoted the MAO coating in providing the higher hardness in comparison to untreated surfaces.

Keywords: Micro arc oxidation, Aluminium alloy, Rock additive, Hardness, wear resistance.

Cite this Article: Samir Hamid Awad, Study on Al_2O_3 Duplex Coatings Deposited by New Micro-ARC Oxidation (MAO) Process Using Natural Additives of Rice Hushes Ash (RHA) and Porcelanite Rocks of Pre-Anodized 6061 Al Alloys, International Journal of Mechanical Engineering and Technology (IJMET)10(2), 2019, pp. 1640–1654.
http://www.iaeme.com/ijmet/issues.asp?JType=IJMET&VType=10&IType=2

1. INTRODUCTION

Aluminum alloys (Al2024, Al6061 and Al7075) are important and widely used, which in particular satisfy the requirements of different space applications with good results and properties [1]. A wide variety of techniques are now available for surface improvement of Al alloys such as chemical conversion coatings , anodic oxidation, laser processing and ion implantation , to modify their surface for heavy load bearing applications [2]. MAO technique, has a significantly advanced in the last two decades as a high –voltage anodizing method, to form a stable, hard and thick Al_2O_3 coatings to enhance the tribological properties of Al alloys [3-8]. MAO process is a multifactor-controlled process, and properties of its coatings can be influenced by many factors, such as electrolytes composition. Many investigations have been done on using different additives for the modification of the MAO electrolytes to improve the coatings mechanical and tribological properties [9-13]. The MAO oxidation method is a complicated process of plasma discharge and anodizing oxidation, and the initially of the MAO method is an anodization method [14]. In anodizing, durable and porous coatings are formed by oxidation and durable surface coating to improve the corrosion resistance of Al surfaces in severely corrosive environments [15-17]. Anodizing is a widely used process, which is distinctive by the good appearance and lower energy depreciation. However, the anodization porous oxide films, cannot have satisfied hardness and anticorrosion performance [2].

In current study, utilization of the effect of "synergy" was applied through the combination of anodic and MAO double coatings. Also, this study is an attempt in using natural additives of Iraqi rock rich with Porcelanite and rice hushes ash (RHA) in modification the MAO electrolyte as an assistant additives for surface modification of pre- anodized Al alloys. Rice husk is considered as an agricultural waste that rich with high content silica (87–97% SiO_2) in an amorphous state, which has been widely utilized in different industries and applications [18 - 19]. Iraqi land is rich of rock materials that contain natural materials like Porcelanite. Porcelanite is one of the important industrial sedimentary rocks contains microcrystalline silica aggregate, with veins of chalcedony and opaque specks [20].

2. EXPERIMENTAL

2. 1. Powders preparation

In this process, rice husk were washed with distilled water, dried at the atmosphere, burned at 800^{o} C for 6 hours, and milled for 12 hours. A suitable amount of Porcelanite rocks were selected from Iraq Geological Survey. Manually kibbling of powders was performed using mortar to get the quasi-finished powder. Then the powders were milled for 8 hours by using ball mill at speed 350rpm. Porcelanite powder was treated at 700^{o}C to convert the carbonate content into oxides. The x-ray diffraction (XRD) and laser particle size analyzer PSA (Type Better size 2000) were used to identify the powder and to characterize particle size.

2.2. Samples preparation

The Al 6063 alloy, with a nominal composition shown in table (1), was selected as the substrate material. Samples (ϕ20x 5mm^2) were ground using SiC paper, to an average roughness of around 1 µm. Then the samples were cleaned with acetone at 25°C, subjected to alkaline etching using 5wt% NaOH solution at 50° C for 5 minutes, and acid etching using 5% HNO3 solution at 25° C for 5 minutes. The samples were cleaned with distilled water, and dried in a drying furnace at 50° C for 30 minutes before the anodization treatment.

Table 1 Al 6063 alloy chemical composition.

Element	Content (wt. %)	Element	Content (wt. %)
Si	0.5	Zn	0.1
Fe	0.3	Cr	0.2
Cu	0.1	Other	0.12
Mn	0.1	Al	Bal.
Mg	0.79		

2.3. Anodizing and micro arc oxidation process

The present study included sulfuric acid anodizing for pretreatment process. The anodization was conducted at constant current density (3.5 A/dm^2) at 19°C for 20 min in a 10 % vol H_2SO_4 solution. When the anodizing process was completed, the samples were dipped in hot distilled water and kept for 20 minutes at 97°C in order to seal the porous anodic film, then they were dried in a drying furnace at 50° C for 15 minutes. For MAO treatment, a 500V DC-AC homemade deposition unit shown in fig. (1) was employed to deposit the ceramic coatings at fixed current density of (6)A/dm^2 and voltage of 390V. In the plastic container, a five litters electrolyte was agitated and cooled using a mechanical stirrer and cooling system, respectively. Also, the plastic container was equipped with a sample holder as the anode and a st st 316L plate serving as the cathode. The cooling unit connected to the MAO unit works to maintain temperature of electrolyte below 30 C. It provides the cooled water to a big plastic container surrounded the electrolyte solution

container. After treatment, the obtained coated samples were washed with distilled water and dried at room temperature. The tables (2) and (3) show the electrolyte composition and deposition parameters. The electrolytic solutions were mixed after preparation for 3 hours before the MAO process.

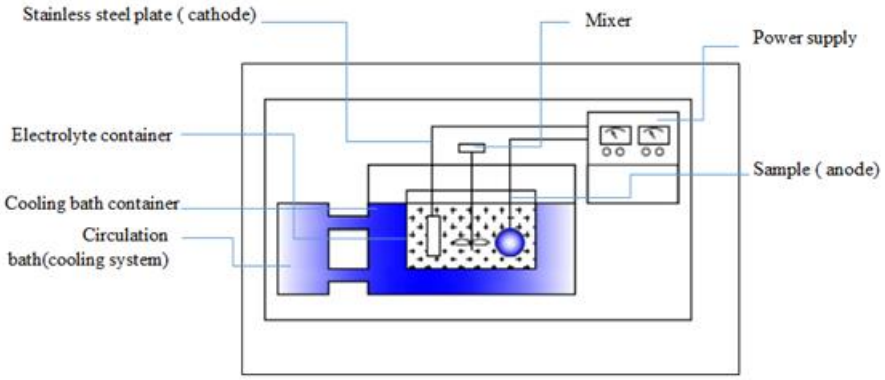

Figure 1 MAO coating equipment

Table 2 Composition of modified electrolytes

Component	Concentration	Specification
KOH	3g/l	Electrolyte conductivity increasing
KH_2PO_4	15g/l	Property modification
Porcelanite	20g/l	Assistance
RHA	20g/l	Assistance

Table 3 Deposition parameters

Sample code	Deposition time (min)
ME_1	10
ME_2	20
ME_3	40
ME_4	60

2.4. Characterization

The Al substrates and powders were characterized using X-ray Diffractometer (XRD-6000SHIMADZU, Japan, Cu Kα radiation, 40Kv, 30MA, 6⁰/min scanning speed). The phase content, surface morphology, structure, and element distribution of the coatings were investigated using XRD- 7000 SHIMADZU system, and scanning electron microscope (INSPECT S50, FEI Company) equipped with energy dispersive spectroscopy (EDS). Micro-hardness was measured by a Vickers indenter (HVS-1000, Laryee, digital Micro-hardness tester) with load of 4.9 N and holding time of 15 seconds. Microprocessor CM-8822, coating thickness, was employed to measure thickness coatings. Surface topography and roughness parameters were obtained using Atomic Force Microscopy (AFM, contact mode, spm AA3000 Angstrom advanced Inc., USA). The wear resistance was tested using (Microtest-28021) and ϕ 6mm carbide pin at load 10N, sliding speed 200rpm, sliding distance 75 mm, and time 15min.

3. RESULTS AND DISCUSSIONS

3.1. XRD and PSA results of powders

The XRD patterns of RHA shown in figure (2), proved the presence of pure SiO_2 powder (JCPDS card No.03-0227) with small amount of Ca (JCPDS card No.01-0735). After 6 h of heating, cristobalite was observed above 800°C with a strong peak at 21.8° and an additional weak peak at around 36° (ICDD PDF No.39–1425). Such phases of the cristobalite can improve the hardness of ceramic coatings when they incorporate in the MAO discharge channels. Also, the cristobalite phases could not present in the RHA fired at 700 °C in our work [21]. Figure (3) indicated that the RHA powder was with mean particles size about (4μm) distributed on the range of (0.3μm -40 μm) because of the high agglomerations occur due to the surface area of the particles. The XRD results of Porcelanite, which scanned in diffraction angle (2θ) from 5° to 5o°, are shown in figures (4). The phases were identified by comparison with standard references pattern from powder file (JCPDS cards). The patterns refereed to the existence of Tridymite (JCPDS card No.42-1401),Dolomite (JCPDS card No.36-0426), Opal-CT (JCPDS card No.77-0217), Quartz (JCPDS card No.46-1045) , Apatite (JCPDS card No.09-0432) , and Cristobalite (JCPDS card No.39-1425).The aforementioned patterns could exhibited intensities and crystal sizes different form those recorded for the porcelanite fired at 900°C [22]. The size of Porcelanite particles shown in figure (5) proved their distribution in the range (0.3 μm -40 μm) with main particle size about (4 μm).

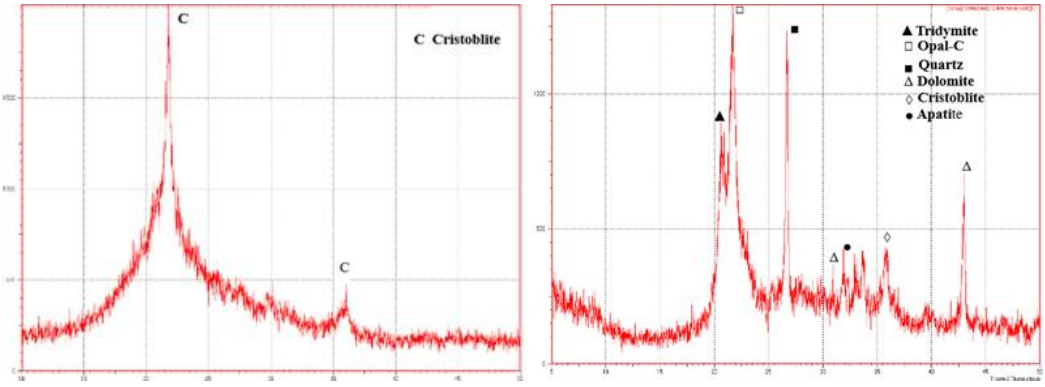

Fig.2. XRD results of RHA powder (800 °C) **Fig.4** XRD results of fired Porcelanite (700°C)

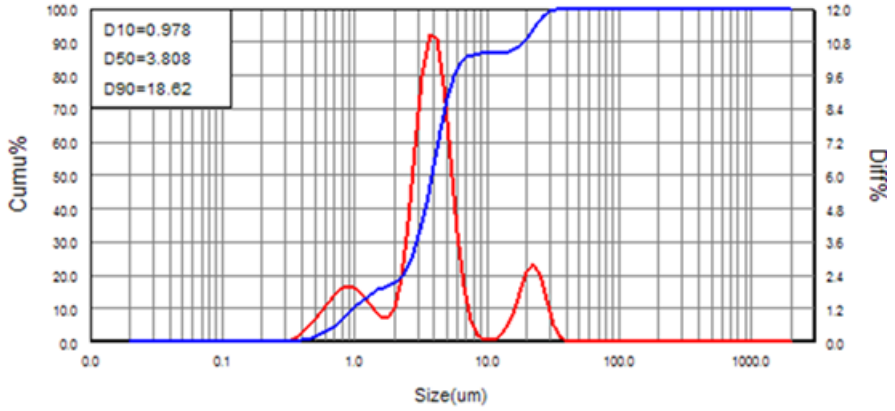

Figure 3 Particle Size Distribution of fired RHA

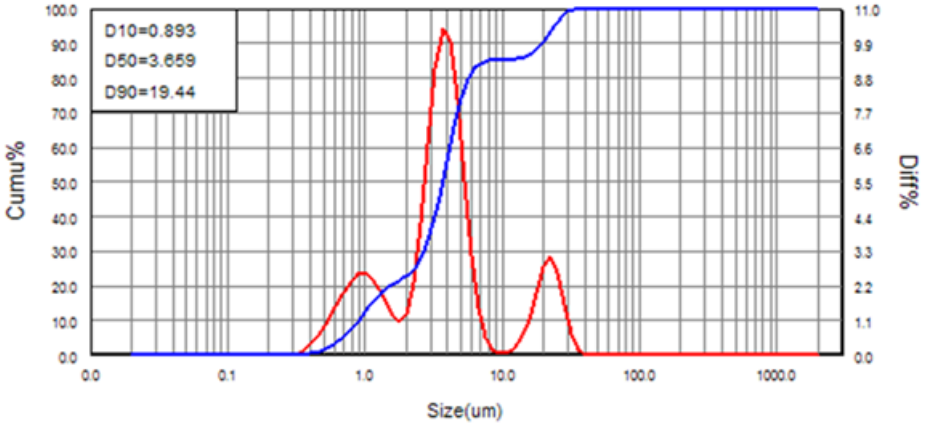

Figure 5 Particle Size Distribution of fired Porcelanite

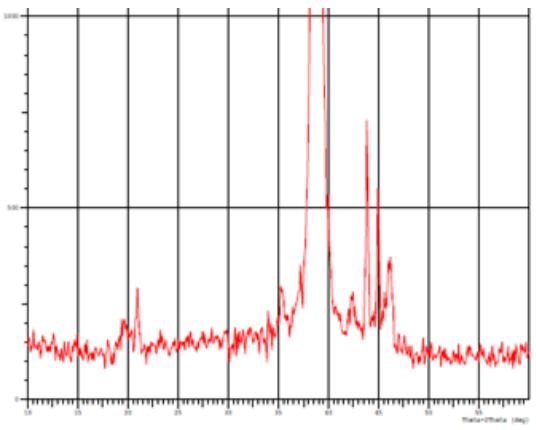

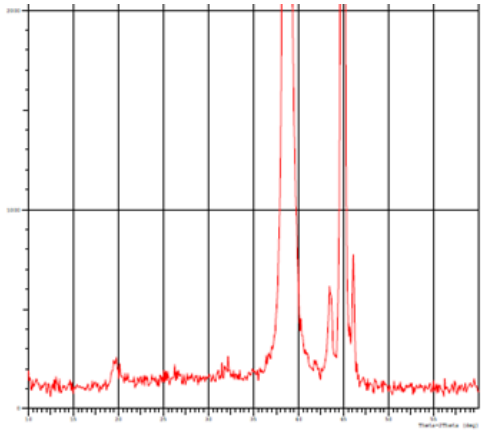

Figure 6 XRD patterns of sample ME_1 **Figure 7** XRD patterns of sample ME4

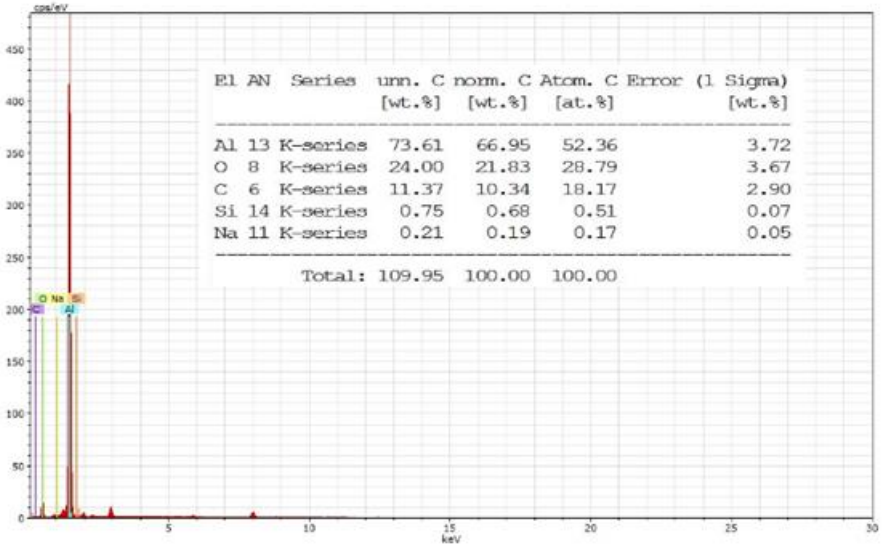

El	AN	Series	unn. C [wt.%]	norm. C [wt.%]	Atom. C [at.%]	Error (1 Sigma) [wt.%]
Al	13	K-series	73.61	66.95	52.36	3.72
O	8	K-series	24.00	21.83	28.79	3.67
C	6	K-series	11.37	10.34	18.17	2.90
Si	14	K-series	0.75	0.68	0.51	0.07
Na	11	K-series	0.21	0.19	0.17	0.05
Total:			109.95	100.00	100.00	

Figure 8 EDS results of sample ME1

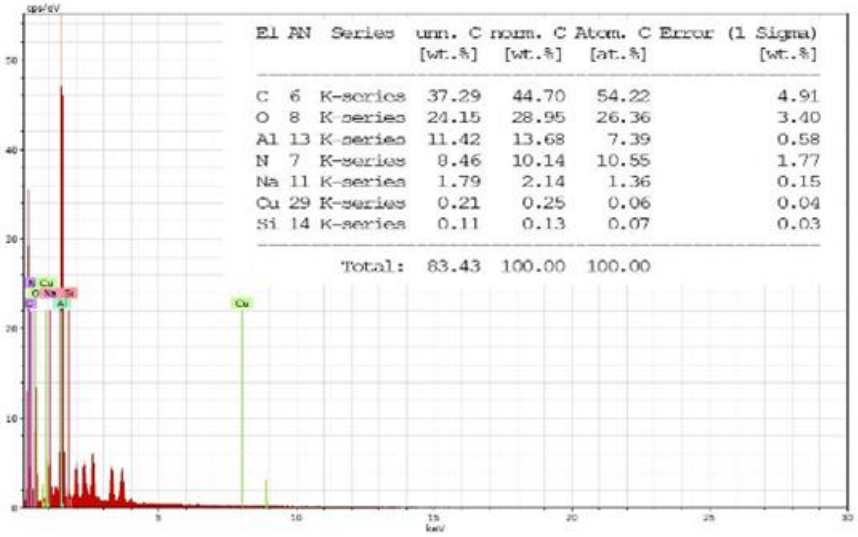

El	AN	Series	unn. C [wt.%]	norm. C [wt.%]	Atom. C [at.%]	Error (1 Sigma) [wt.%]
C	6	K-series	37.29	44.70	54.22	4.91
O	8	K-series	24.15	28.95	26.36	3.40
Al	13	K-series	11.42	13.68	7.39	0.58
N	7	K-series	8.46	10.14	10.55	1.77
Na	11	K-series	1.79	2.14	1.36	0.15
Cu	29	K-series	0.21	0.25	0.06	0.04
Si	14	K-series	0.11	0.13	0.07	0.03
Total:			83.43	100.00	100.00	

Figure 9 EDS results of sample ME2

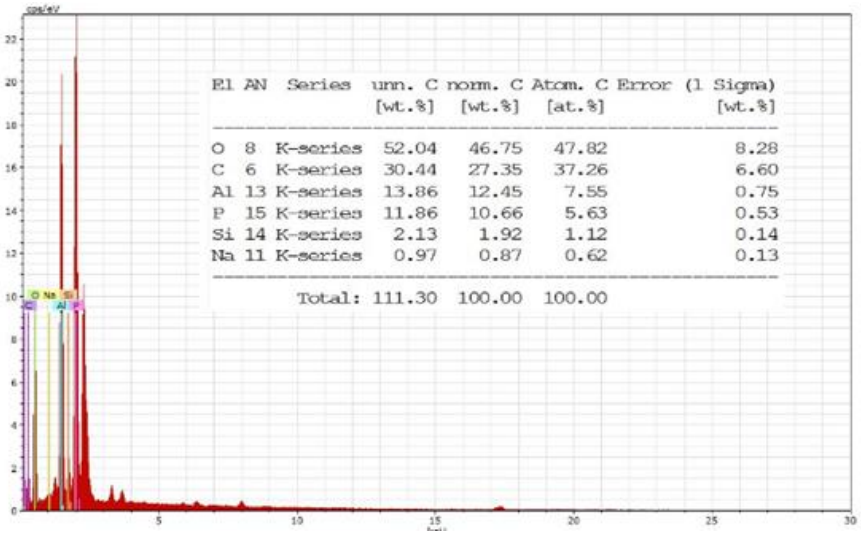

Figure 10 EDS results of sample ME3a

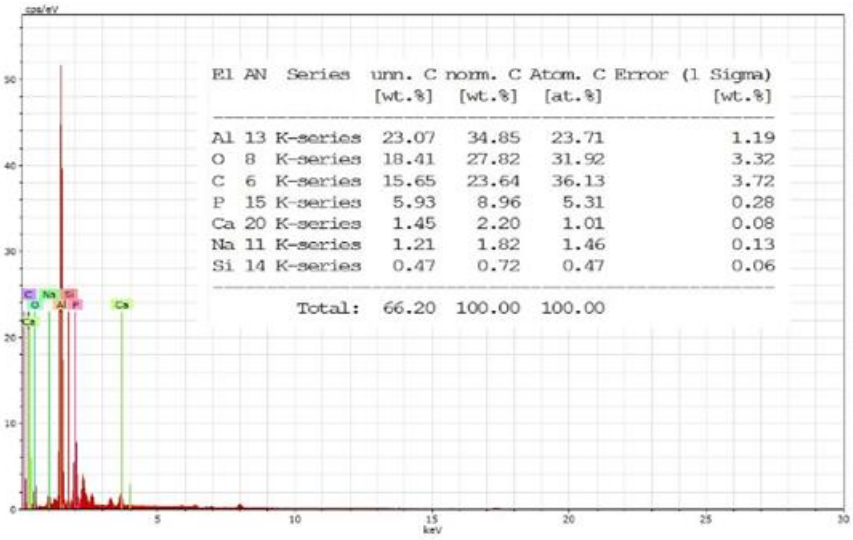

Figure 11 EDS results of sample ME4

3.1. XRD results

Figs. (6) and (7), show the XRD results of the coated samples. XRD patterns proved the deposition of aluminum oxide on the surface of substrates. The mean peaks were γ- Al_2O_3 (JCPDS No. 010-0425). The trimmed peaks with the strongest intensities refer to Al peaks (JCPDS No. 004-0787). Furthermore, such observed peaks can be attributed to the thicknesses and Al peaks coming from the underlying substrate were detected due to the X-rays penetration into the Al substrates.

3.2. EDS results

EDS results given in figures (8–11) could proved the deposition of aluminum oxide. The existence of Aluminum (Al) and Oxygen (O) elements in the coatings, referred to the Al_2O_3 layers formation with different weights of modification elements of C, P, Ca, Si and Na. Generally, C element is always precipitated in the MAO electrolytes, deposited as contaminate, and detected on the unpolished coatings. Furthermore, other elements may be resulted from the contaminates in hydroxyapatite and $CaCO_3$. Also, P is belonged to the chemical compounds used in preparation of the electrolytes. Generally, different elements used in preparation of

electrolytes could react with Al of substrate to produce complex compounds, may also be alloyed within the MAO sparks , leading to the high content of such elements on the deposited coatings. Also, The MAO discharge canals can form a highly porous films, and any components and modifying elements in the electrolytes can be incorporated into oxide films by the discharge.

3.3. Results of SEM

Figures (12- 13) show the surface morphology results from SEM for the coated sample at different magnifications. The morphologies can be observed are characterized by different sizes of sphere-like geometry pores in the structure. These coatings have a pan-like structures with a nonuniformly distributed porous structures. At the discharge spots sites, the metal from substrate and its oxide are melted and projectile over from discharge tunnels due to the very high temperatures at those sites. The observed pan-cake-like morphology is resulted from the molten liquid that quickly solidified leaving distinct boundaries around the pores. Also, such rapid solidification induced the microcracks appearance on the morphology due to molten oxide continuous exposing to cold electrolyte. Furthermore, An observed feature of the MAO process using the natural additives containing electrolytes was a plasma discharge that occurred at the metal/electrolyte interface when the applied voltage exceeded 280V (a critical breakdown voltage) and appeared as a short-lived micro discharges moving across the metal surface. Then, the electrolytes could clearly show the normal & continuous sparks movement at 390 V and 6 A/dm^2 current density. The spark movement can be attributed to the deposition of substrate, and spot localized healing with the subsequent sparking at weak spots in the coating. In general, sample ME_2 (at 20 min) showed structure characterized by pores non-uniform distribution and their different sizes. Considering such non-uniform distribution of porosity, it could have its effects in lowering the hardness of sample ME_2 in comparison with other samples. In general, the hardness differences is strongly attributed to the non-uniform distribution of pores in coatings. The structure of ME_4 was characterized by, relatively low pores with uniform distribution, which has its effects on the increasing hardness values.

3.4. Thickness and Hardness results of coatings

Table (4) and figures (16-17) presents the results from thickness, hardness, and surface roughness. The hardness values of the coating are 350-513HV, which are higher than that of the substrate (75. ±2 HV). The coating is mainly composed of γ-Al2O3, were a proportion of 60% γ-Al2O3 in coatings exhibits high hardness [23]. The preanodized treatment could provide 13-17 μm ceramic coatings with hardness of 190 Hv. In general, double- layer coatings deposited by anodizing and MPO processes using rice hushes ash (RHA) and porcelanite rocks natural additives containing MAO electrolytes could improve the Al substrates with thick and hard ceramic alumina in comparison to untreated coatings. The highest hardness value(535HV) recorded at 60 min deposition time, proves the combined effect of fired porcelanite at 700 ^{o}C RHA fired at 800 C in providing improved hardness values in comparison to those obtained in our previous works [22] after addition of fired porcelanite (900^{o}C) , with and without nano particles of TiO_2 and Na_2WO_4.Also, such improved hardness values can be acceptable in comparison to those recorded after using fired RHA (700^{o}C)in our previous work [23]in modification of MAO electrolytes. Anodizing permanently changes the outer structure of the oxidized surface, and make it much thicker, up to several micrometers. The anodized aluminum oxide coating is very hard, The porous nature of oxidized surface makes it possible to impregnate such pores with the number of discrete short-lived micro discharges moving across the Al surface during the subsequent MAO process. The variation of coatings thickness with deposition time can be attributed to the broken of weak oxide layer by strong spark during growth, thereby, forms different thickness values. It can be concluded that the thickness values

were (60-90) μm, and the sample ME_4 exhibited the highest value (90 μm) at 60 min in comparison with the other coatings. While sample ME_1 recorded the lowest (60μm) thickness at 10min.Generally, the increasing of coating thickness can be observed with deposition time increasing. It is interested to mention that, only the micro-hardness test at 4.9 N and holding time (15sec) could evaluated the coating hardness.

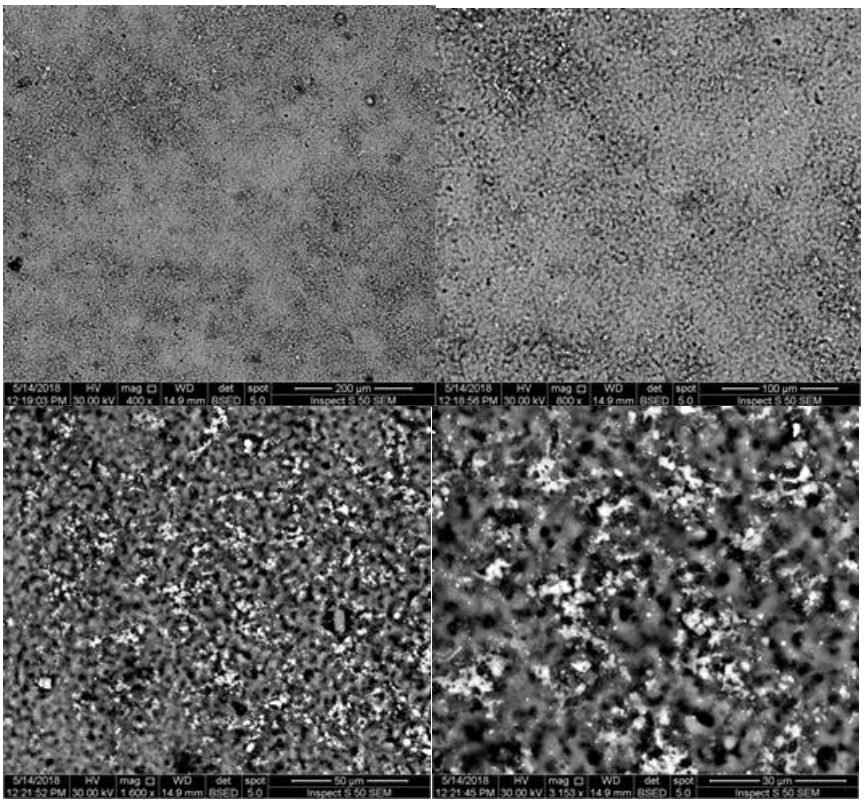

Figure 12 Surface morphology results from SEM observation of sample ME1 at different magnifications.

In general using loads of (50, 100, 150, 250, 350,400) g could not show any track in the coating surface. The dense layer exhibited the higher value of hardness, while the hardness of porous layer was rather low. It can be observed that the sample ME_1recorded the lowest (400 HV) hardness because of their porous structures characterized by more nonuniform pores distribution in ceramic oxide pointed in SEM results. The ceramic coatings showed surface roughness in the range (1.57-10.4) μm. Generally, the coating roughness decreased with deposition time increasing.

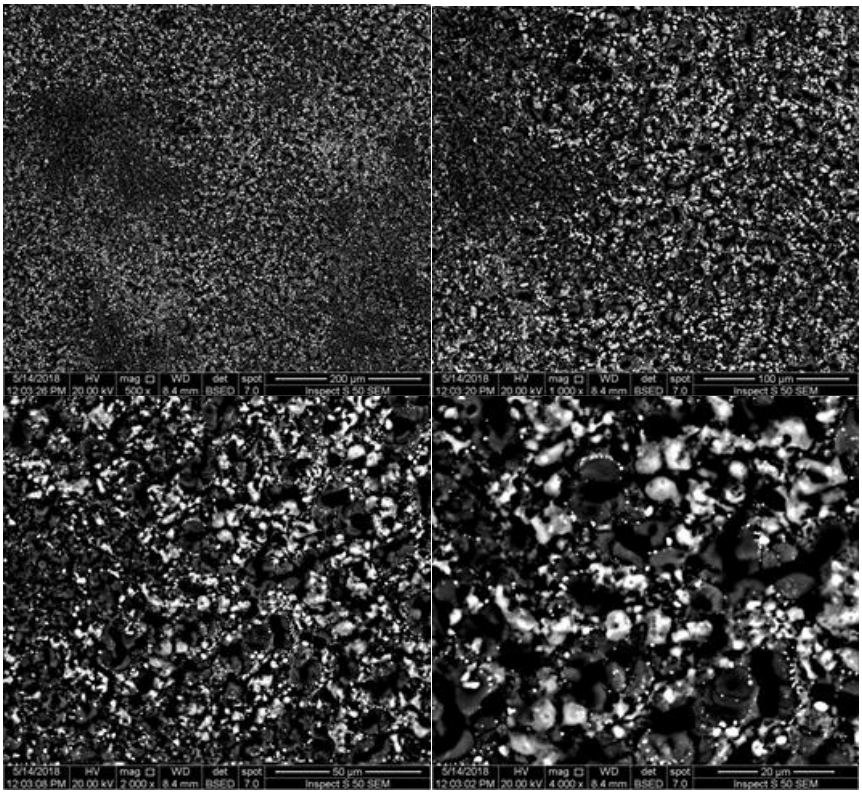

Figure 13 Surface morphology results from SEM observation of sample ME2 at different magnifications

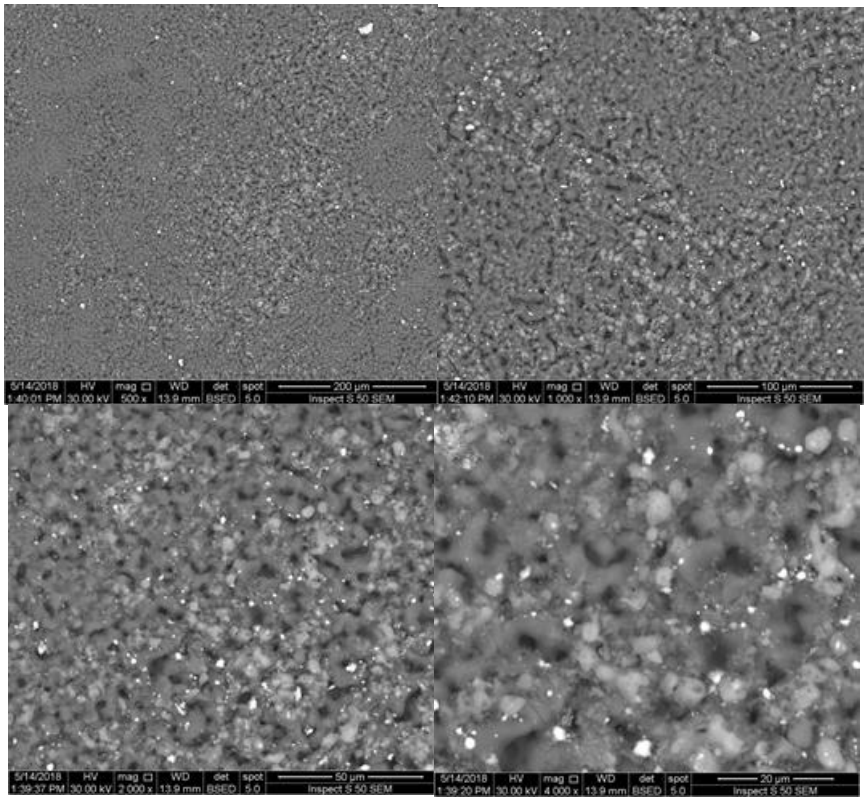

Figure 14 Surface morphology results from SEM observation of sample ME3at different magnifications

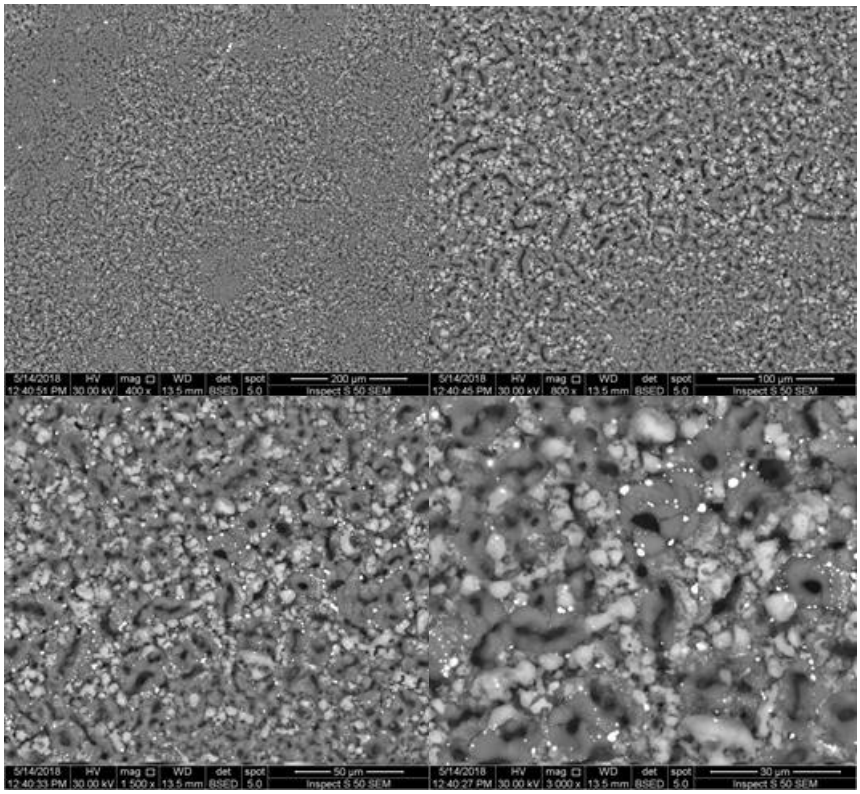

Figure 15 Surface morphology results from SEM observation of sample ME4 at different magnifications

Sample	Thickness (μm)	Hardness (HV)		Roughness (μm)
		Un pretreated	Preanodized	
ME_1	60	350	400	10.4
ME_2	67	410	470	5.49
ME_3	82	450	485	1. 57
ME_4	90	500	535	8.88

3.5. AFM results

AFM images of the coatings surfaces are presented in Fig. (19) and the corresponding roughness values measured on 3D topographies, are shown in Table 4. It can be noticed from Fig. 14 that the ceramic coatings showed surface roughness in the range (1.57-10.4) μm. Generally, the coating roughness decreased with deposition time increasing to 30 min, then the thick coatings of sample ME4 exhibited the surface roughness at about (8.88) μm . AFM results could indicate that the coatings were characterized with cluster of particles and dense structure, the particles were closely bonded, and no voids were observed in samples. Anyhow, the voids appeared in the topographies of sample ME_4, proved the surface roughness increasing with the increasing of deposition time to 60 min.

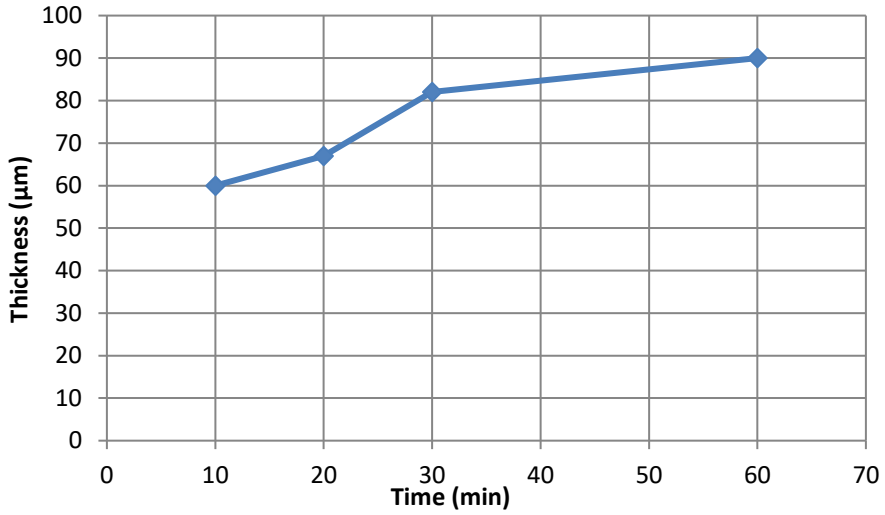

Figure 16 Effect of deposition time on coatings thickness

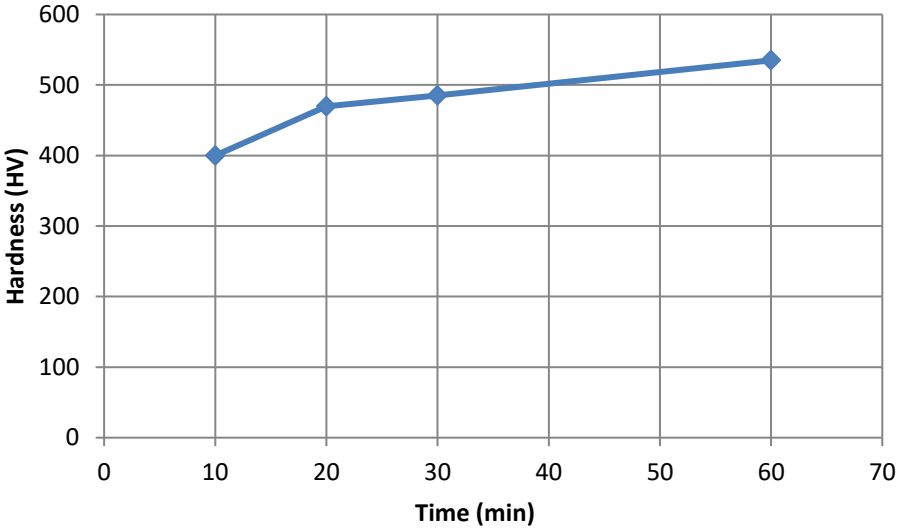

Figure 17 Effect of deposition time on coatings hardness

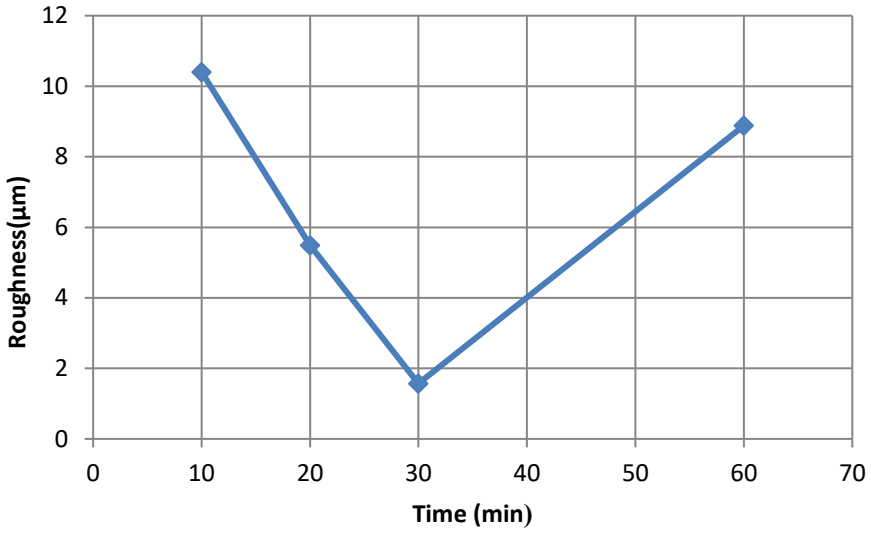

Figure 18 Effect of deposition time on coatings roughness

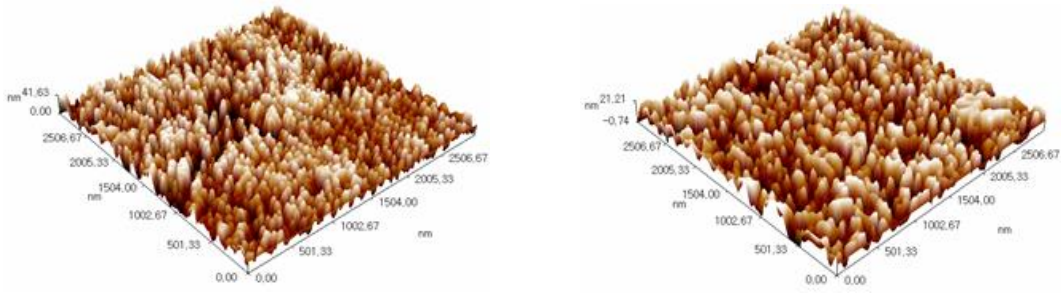

(a): Ra=10.4 (b): Ra=5.49

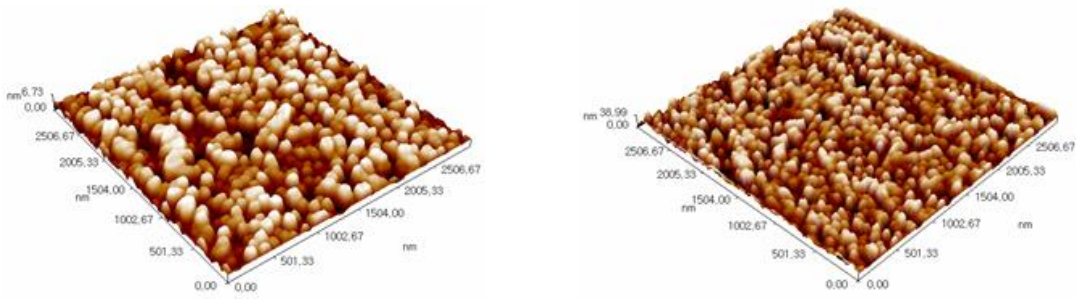

(c): Ra=1.57 (d): Ra=8.88

Figure 19 AFM results of the coated samples

3.5. Wear results

The pin- on disc sliding wear measurements were carried out to determine the wear rate which expressed by means of mass loss with an accuracy of 0.1mg. Coated and uncoated samples were carefully cleaned, and the weight was measured before and after a wear test. The values of weight loss are shown in table (5). The results could prove that the pretreatment of anodizing and the using of fired porcelanite rock additives and RHA additives can be a promising process

to modify the MAO electrolytes for surface improvement of Al alloys to deposit oxide layers with good wear resistance. Furthermore, the coated samples had weight loss of ($7x10^{-4}$-$12x10^{-4}$) g, while the Al substrate had weight loss of ($42x10^{-4}$) g. Also, it can be observed that the wear rate decreased with the increasing of deposition time due the thick coating which prompted the wear resistance in severe load condition.

Table 5 Wear results

Samples	Weight loss (g)
Substrate	$42x10^{-4}$
ME_1	$12x10^{-4}$
ME_2	$10x10^{-4}$
ME_3	$9x10^{-4}$
ME_4	$7x10^{-4}$

4. CONCLUSION

The presented work showed the process and characterization of ceramic coating deposition on preanodized Al 6061 alloy by MAO process using natural additives modified electrolytes. The results confirmed that the pretreatment of anodizing and using of new MAO electrolytes modified by RHA and porcelanite natural rock additives can be used to deposit hard (400-535HV) and thick (60-90μm) γ-Al_2O_3 coatings on Al alloy substrates. The structures of these coatings were characterized by different size of pores and their distributions. Moreover, hardness differences were strongly affected by the non-uniform distribution of pores and increased with increasing of deposition time. Also, the AFM results showed an average roughness in the range (1.57-10.45 μm) which decreased with increasing of deposition time to 40 min, then showed maximum value at 60 min due to the highest coating thickness. The most key feature of the double coatings and new electrolyte used in the present study is the wear resistance improvement by means of weight losses.

REFERENCES

[1] Afaf M. Abd El-Hameed, Yehia A. Abdel-Aziz, Fatma S. El-Tokhy, 2017. Anodic Coating Characteristics of Different Aluminum Alloys for Spacecraft Materials Applications. Materials Sciences and Applications. 8, 197-208.

[2] Xuping Zhao, Dan Liu, Jieqin Lu, Guoying Wei, 2017. Micro-arc Oxidation Coating Formed on Anodized Aluminum Surface under Different Pulse Frequencies. Int. J. Electrochem. Sci., 12**:** 7922 – 7930.

[3] T. W. Clyne and S.C. Troughton, 2019. A review of recent work on discharge characteristics during plasma electrolytic oxidation of various metals. J International Materials Reviews 64, 3: 127-162**.**

[4] Y Zhang, Y Chen, H Q Du and YW Zhao, 2018. Corrosion resistance of micro-arc oxidation coatings formed on aluminum alloy with addition of Al2O3. Materials Research Express, 5, 3**.**

[5] S. Lederer, P. Lutz, W. Fürbeth," Surface modification of Ti 13Nb 13Zr by plasma electrolytic oxidation" Surface & Coatings Technology, 2017, 257-8972, 62-71.

[6] A. Soboleva, A. Kossenkoa, M. Zinigrada and K. Borodianskiya," Comparison of Plasma Electrolytic Oxidation Coatings on Al Alloy Created in Aqueous Solution and Molten Salt Electrolytes" Surface & Coatings Technology,2018, 30342-6.

[7] Y. Zhang, W. Fan, H.Q. Du, Y.W. Zhao, 2017. Corrosion Behavior and Structure of Plasma Electrolytic Oxidation Coated Aluminum Alloy. Int. J. Electrochem. Sci., 12**:** 6788 – 6800.

[8] Hong Li, and Jin Zhang,2017. Preparation of a Modified Micro-arc Oxidation Coating Using Al2O3 Particles on Ti6Al4V. Journal of Material Sciences & Engineering, J Material Sci Eng, 6:6.

[9] H. Nasiri Vatan, R. Ebrahimi-Kahrizsangi, M. Kasiri Asgarani, 2016. Effect of WC Nano-powder on Properties of Plasma Electrolytic Oxidation coating Fabricated on AZ31B Alloy. International Journal of electrochemical science 11: 929 – 943.

[10] Mohammadreza Daroonparvar, Muhamad Azizi Mat Yajid, Noordin Mohd Yusof, 2016. Preparation and corrosion resistance of a nanocomposite plasma electrolytic oxidation coating on Mg-1%Ca alloy formed in aluminate electrolyte containing titania Nano-additives. Journal of Alloys and Compounds.

[11] S.K. Kiselyeva, L.I. Zaynullina, M.M. Abramova, N.Y. Dudareva and I.V. Alexandrov, 2014. The Effect of Micro arc Oxidation (MAO) Modes on Corrosion Behavior of High-Silicon Aluminum Alloy. Journal of Engineering Science and Technology Review 7:36-39.

[12] Hong-yan Ding a, Zhen-dong Dai b, Suresh C. Skuiry c, David Hui, 2009. Corrosion wear behaviors of micro-arc oxidation coating of Al2O3 on 2024Al in different aqueous environments at fretting contact. Tribology International 43 (2010) 868–875.

[13] Pezzato, L., Angelini, V., Brunelli, K., Martini, C., and Dabala, M. (2018). Tribological and corrosion behavior of PEO coatings with graphite nanoparticles on AZ91 and AZ80 magnesium alloys. Transactions of Nonferrous Metals Society of China, 28(2), 259-272.

[14] R.O. Hussien, and D.O. Northwood, 2014. Production of anti-corrosion coatings on light alloys (Al, Mg, Ti) by plasma-electrolytic oxidation (PEO).PhD. Thesis, Developments in Corrosion Protection, http:// dx.doi.org/10.5772/57171.

[15] K. labisz, J. Konieczny, Ł. Wierzbicki, J. cwiek , and A. butor , 2018. Influence of Primary Silicon Precipitates On Anodized Aluminum Alloys Surface Layer Properties. Transport Problems 13 (2), 111-120.

[16] Sami A. Ajeel , Nahidh W. Kasser , and Basheer A. Abdul-Hussein, 2010. Breakdown and Pitting Formation of Anodic Film Aluminum Alloy (3003). Modern Applied Science Vol. 4, No. 5; 87-101.

[17] Teng-Shih Shih, Tin-Hou Lee and Ying-Jhe Jhou, 2014. The Effects of Anodization Treatment on the Microstructure and Fatigue Behavior of 7075-T73 Aluminum Alloy. Materials Transactions, Vol. 55, No. 8 pp. 1280 – 1285.

[18] Midhun Dominic C.D, P.M Sabura Begum, Rani Joseph, Daisy Joseph, Prabith Kumar, and Ayswarya E.P,2013. Synthesis, characterization and application of rice husk nano-silica in natural rubber. International Journal of Science, Environment and Technology, Vol. 2, No 5,pp. 1027–1 035.

[19] Yasushi SHINOHARA, and Norihiko KOHYAMA. 2004, Quantitative Analysis of Tridymite and Cristoblite Crystallized in Rice Husk Ash by Heating. Industrial Health, 42, 277–285

[20] Jabboory, W.M,1999. Mining geology of the porcelanite deposited in wadi Al-Jandali-western desert Iraq. M.Sc. thesis, College of Science, University of Baghdad.

[21] Noor Fadhil Sultan Al-Dulamy, and Samir Hamid Awad Al-Rubay,2017. Effects of rice husks ash addition on alumina layers deposited on 2024 Aluminum alloys by micro-arc oxidation (MAO). Advances in Natural and Applied Sciences.11(1):19-30.

[22] Farqad Saleem Murad, Samir Hamid Awad, and Elham Abdeamajeed, 2018. Effects of natural rock and nano-TiO2 additives on layer deposited on Al Alloys by Micro-arc oxidation (MAO). Journal of Eng.and Applied Sciences 13(5):1201-1209.

[23] Student, Dovhunyk V, Klapkiv D, Posuvailo V, Shmyrko VV, Kytsya .2012. Tribological properties of combined metal-oxide–ceramic layers on light alloys, Mater. Sci. 48, 180–190